Vol. 16, No. 46, Spring 2026, Pages 17-30

Journal of Analytical and Numerical Methods in Mining Engineering

Journal home page: http://anm.yazd.ac.ir/

Research article

Stability Analysis of Intersection Resulted from Slope and Access Tunnels in Tabas Coal Mine using Finite Difference Numerical Method

Alireza Tarakameh[1], Satar Mahdevari[1*], Kourosh Shahriar[1]

1- Dept. of Mining Engineering, Amirkabir University of Technology, Tehran, Iran

(Received: 21 October 2024, Revise: 27 May 2025, Accepted: 28 May 2025)

DOI: 10.22034/ANM.2025.22282.1646

Keywords

Bifurcation
Stability analysis
Induced stress
Plastic zone
Finite difference method
Parvadeh Tabas coal mine

English Extended Abstract

Summary

The demand for underground infrastructures has increased significantly in recent decades due to urbanization, industrial needs, and mineral extraction. In coal mining, the design and construction of intersecting tunnels, especially bifurcated intersections, pose unique challenges. These intersections are often subject to complex stress redistribution, displacement, and plastic deformation. Failure to address these conditions can jeopardize the overall stability and safety of the mining operation.

This study presents a numerical investigation into the stability of a bifurcated tunnel intersection (H16) in the Parvadeh coal mine, Tabas, South Khorasan, Iran. The intersection, formed by S2 slope tunnel and MG5 access tunnel, is situated at a depth of 570 m, within a geologically complex and mechanically heterogeneous rock mass. The Finite Difference Method (FDM), implemented in FLAC3D, was used to model excavation sequences, stress redistribution, plastic deformation, and the effectiveness of proposed support systems. A sensitivity analysis examined the influence of critical geotechnical parameters. Results highlighted key areas of instability, optimal reinforcement strategies, and practical implications for mine design. Field validation also confirms the reliability of the numerical model.

Introduction

With the continuous advancement of society, the need for the construction of underground structures has significantly increased. Depending on the function of the civil structure or the mine design, some tunnels are inevitably excavated in an intersecting manner. With the growing reliance on underground resources and infrastructures, the stability of complex tunnel has gained strategic importance. One type of intersecting tunnel is the bifurcated tunnel, whose stability analysis is of particular importance due to its complex geometric conditions and induced stresses [1]. The span width of bifurcated tunnels at the intersection point is generally greater than that of the regular tunnel section, which leads to increased displacements and reduced structural stability at the intersection. Tunnel intersections are highly vulnerable to instability, which can compromise operational safety and lead to significant economic losses. Therefore, any instability occurring at the tunnel intersection can affect the overall structural stability, making it a critical issue from an engineering perspective [2].

In this study, the stability of a bifurcated intersection in the Parvadeh coal mine—formed by the intersection of S2 slope tunnel and MG5 access tunnel—is investigated as a case study. The aim of this research is to analyze the structural stability at the bifurcated intersection by examining the induced stress field, the

*Corresponding author: E-mail: satar.mahdevari@aut.ac.ir

Vol. 16, No. 46, Spring 2026, Pages 17-30

Journal of Analytical and Numerical Methods in Mining Engineering

Journal home page: http://anm.yazd.ac.ir/

intensity of stress concentration, and the extent of the plastic zone around the intersection area.

Methodology and Approaches

Numerical modeling was carried out using the FDM within the FLAC3D software environment. Figure 1 presents the geological column of the study area. The tunnel cross-section in the bifurcated intersection zone mainly consists of sandstone, siltstone, and silty-sandstone layers, with the C2 coal seam also observed in the roof. As shown, the H16 bifurcated intersection is characterized by a wide cross-section and an asymmetric geometry, connecting the S2 slope tunnel to the MG5 access tunnel at an angle of 78 degrees at a depth of 570 m. Due to the mine design and ongoing extraction operations, various structures are located around the H16 bifurcated intersection. The excavation of each tunnel disturbs the in-situ stress field, resulting in overlapping induced stresses. Moreover, the considerable depth of this intersection generates relatively high in-situ stresses, with the vertical stress reaching up to 15 MPa. Additionally, the inclination angle of the S2 slope tunnel is about 15 degrees from the horizontal, while the MG5 access tunnel has an inclination angle of approximately 6 degrees. To ensure that the modeling conditions closely resemble the actual ground conditions, the model dimensions were selected in such a way that the influence of boundary conditions on the overall model behavior is minimized. The physical and mechanical properties of the rock layers within the study area are summarized in Table 1.

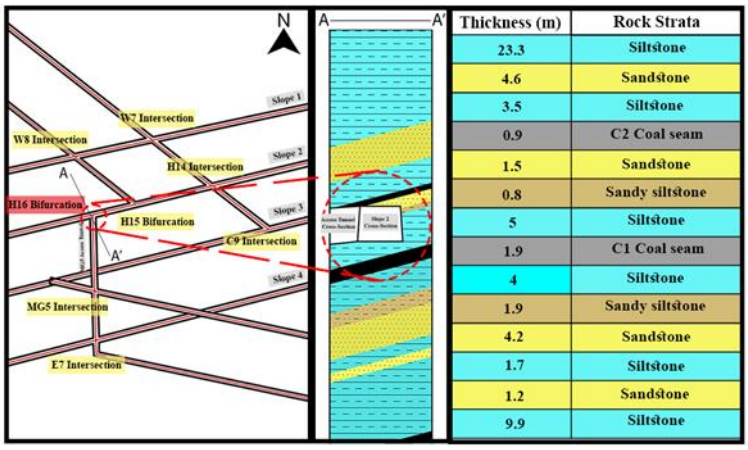

Fig. 1. Geological cross-section of the H16 intersection area

Table 1. Geomechanical and physical properties of rock strata in the study area

Rock Strata	Unit weight $(^{kg}/_{m^3})$	Modulus of deformation (GPa)	Cohesion (MPa)	Friction angle (deg)	Poisson's ratio
Siltstone	2400	1.268	0.72	18.23	0.25
Sandy siltstone	2600	2.167	0.21	27.05	0.25
Sandstone	2700	2.164	1.22	27.03	0.25
Coal seam	1600	0.621	0.43	11.83	0.32

Given that the maximum tunnel span at the intersection is 6.9 m, based on Saint-Venant's principle, the model dimension in the Y-axis direction was chosen to be five times the tunnel width on each side, resulting in a total width of 70 m. The model length along the X-axis, which aligns with the tunnel advance direction, was set to 100 m, with the intersection located at the center of this axis. The model height in the Z-direction was

Vol. 16, No. 46, Spring 2026, Pages 17-30

Journal of Analytical and Numerical Methods in Mining Engineering

Journal home page: http://anm.yazd.ac.ir/

also set to 100 m, incorporating 30 m below and 70 m above the intersection to account for immediate roof and floor interactions.

Groundwater effects were not considered in the analysis, and only in-situ stresses were applied as initial conditions. The overburden weight was modeled as vertical stress acting on the top boundary, while the side boundaries were fixed against horizontal displacement, and the bottom boundary was fixed against both vertical and horizontal displacements. Additionally, the horizontal-to-vertical stress ratio was set to 1.15, and the Mohr–Coulomb failure criterion was adopted to simulate the mechanical behavior of the surrounding rock mass.

The support system of the slope tunnel consists of 22 mm diameter rock bolts with a length of 2.4 m, arranged in a regular pattern with 1-meter spacing. These bolts are fully grouted with resin and installed in combination with wire mesh. In addition, sliding steel frames of type TH36 are used at 800 mm intervals to ensure the stability of the S2 slope tunnel; the space between the steel frames and the tunnel wall is filled with backfill material. The mechanical properties of the support systems are summarized in Table 2.

Table 2. Specifications of the proposed support system

Parameter	Unit	Roof Anchor Cable	Roof flexibolt	Rock bolt
Diameter	(mm)	42	21.7	22
Length	(m)	9	6	2.4
Tensile Strength	(kN)	590	490	310
Compressive Strength	(kN)	–	–	250
Pretension	(kN)	250	–	–
Allowable Strain	(%)	–	–	18
Anchorage Length (Bond)	(m)	5	4	2.4
Grouting Material		Grout	Resin	Resin

As the slope tunnel approaches the intersection, due to the increased span and cross-sectional area, a reinforced support system is employed. Specifically, within a 9-meter radius from the center of the intersection, denser-patterned rock bolts with a length of 2.7 m are installed in the slope tunnel. At the intersection itself, the support system includes 9-meter prestressed anchors, 6-meter flexibolts, and rock bolts spaced at 800 mm intervals.

Due to the increased cross-sectional area at the bifurcated intersection, IPB260 and IPB320 beams were used instead of sliding steel frames. The arrangement of grouted rock bolts in the roof and walls of the access tunnel follows a square pattern with 800 mm spacing. Additionally, 6-meter flexibolts were installed in the roof, and IPB260 steel frames were also used as part of the support system in this tunnel.

Results and Conclusions

Nephogram showing the distribution of vertical stresses in the right wall of the slope tunnel is presented in Figure 2. As observed, the vertical stress initially increases with distance from the right wall of the slope tunnel and begins to decrease at approximately 14 m from the center of the intersection, eventually stabilizing. The maximum vertical stress in the stress concentration zone reaches 25.5 MPa. By comparing the contour lines around the tunnel cross-section, it is evident that the stress concentration at the intersection is effectively controlled through the installation of the proposed support system.

*Corresponding author: E-mail: satar.mahdevari@aut.ac.ir

Vol. 16, No. 46, Spring 2026, Pages 17-30

Journal of Analytical and Numerical Methods in Mining Engineering

Journal home page: http://anm.yazd.ac.ir/

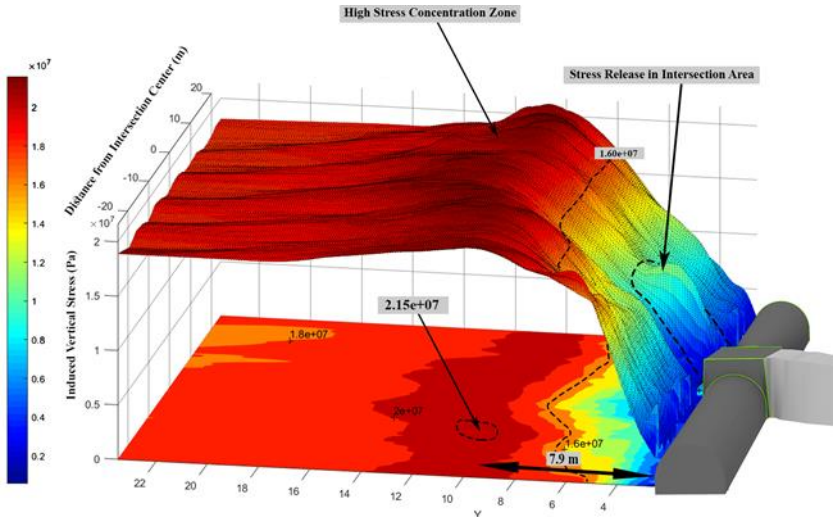

Fig. 2. Nephogram of vertical stresses in the right wall of the slope tunnel

With increasing distance from the bifurcated intersection, greater stress concentration occurs in the access tunnel. For greater clarity, a 3D view of the induced vertical stresses on both sides of the bifurcated intersection is shown in Figure 3. According to the stress distribution curves, the vertical stress levels in the rock mass on the left side—where the intersection angle is smaller—are significantly higher than on the right side. Moreover, the zone of maximum induced vertical stress on the left side occurs closer to the sharp corner of the intersection compared to its counterpart on the right. Additionally, both the peak value and the extent of the area with more intense stress distribution are greater on the left side.

Also, based on the stress concentration contours in the area between the slope tunnel and the access tunnel, on the left side of the bifurcation, the stress concentration was increased to 1.65 near the slope tunnel, and to 1.71 near the access tunnel. Moving away from the intersection at the roof of the access tunnel, the stress level increases, which can be due to its non-circular and wide cross-section. Overall, the trend of induced vertical stress initially increases continuously, then decreases with increasing distance from the intersection, and finally stabilizes. This distribution forms dome-shaped iso-stress contours with a peak value at the center, gradually diminishing as the dome expands.

Based on the shear stress curves in the rock mass on the left side of the intersection, the shear stress reaches 7.98 MPa at a distance of approximately 12 m from the sharp corner of the intersection (Figure 4a). Additionally, within 2 m of this corner, the shear stress field increases to 5.87 MPa. Overall, it can be concluded that the intensity of shear stress concentration is higher in the rock foundation on the left side. According to Figure 4b, the shear stress on the right side of the bifurcated intersection reaches 7.11 MPa at a distance of 11.3 m from the corner. Furthermore, the trend of shear stress variation in the rock mass on the right side increases in the direction of the access tunnel. In contrast, the shear stress distribution in the left-side rock mass tends to be more symmetrical relative to both the slope tunnel and the access tunnel.

Vol. 16, No. 46, Spring 2026, Pages 17-30

Journal of Analytical and Numerical Methods in Mining Engineering

Journal home page: http://anm.yazd.ac.ir/

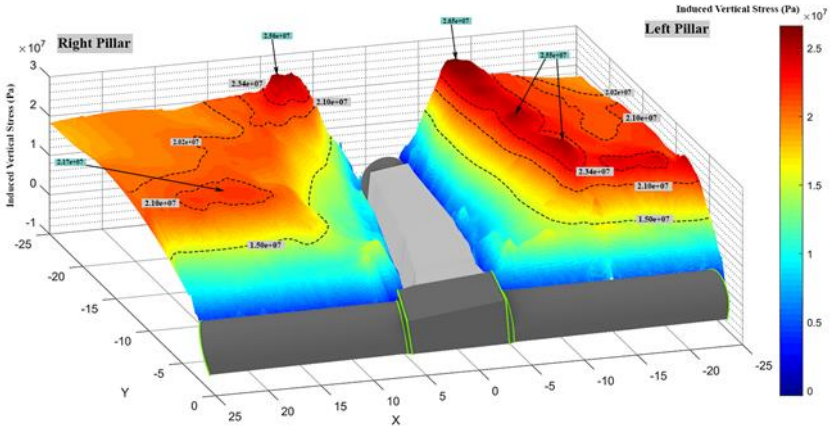

Fig. 3. 3D view of induced vertical stresses on both sides of the bifurcated intersection

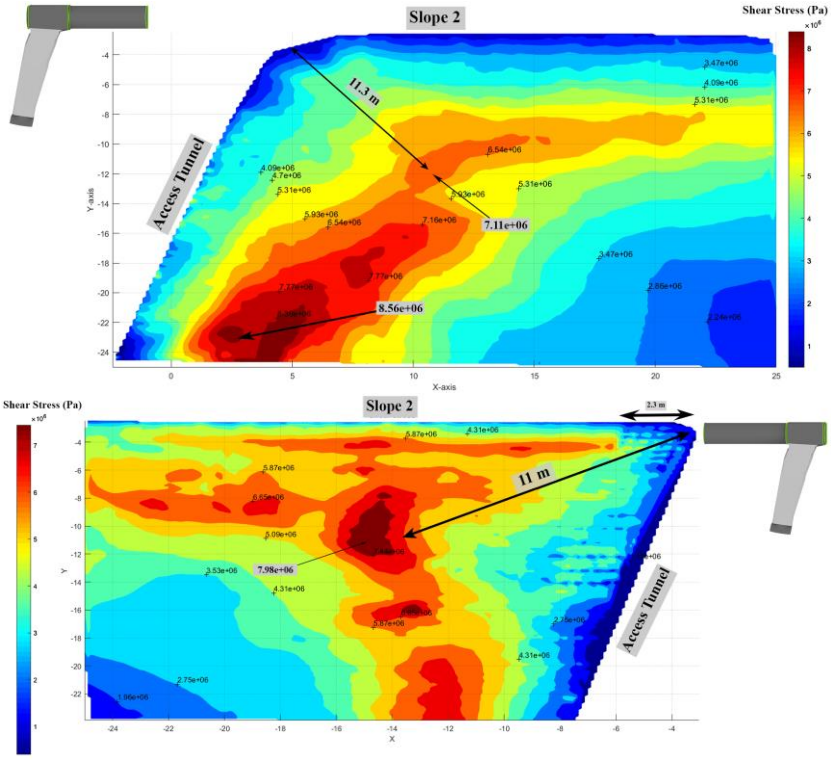

Fig. 4. Shear stress variation curves in the zone between slope tunnel and access tunnel (plan view)

The extent of the plastic zone in four areas of tunnel roof, tunnel floor, right wall, and left wall decreases with increasing distance from the center of the intersection. However, the depth of the plastic zone is greater in the left wall of the slope tunnel. Similarly, in the access tunnel, the spread of the plastic zone—particularly in the walls—continuously decreases as the distance from the intersection increases.

Due to the existence of rock strata with different strengths, the plastic zone at different distances from the intersection is almost asymmetric. This phenomenon is illustrated in Figure 5, which shows the positioning of a weak coal seam located 20 m from the intersection. By comparing various distances and the relative position of the coal seam to the excavation profile, it can be concluded that the plastic zone is smaller when the weak layer lies in the roof of the excavation, compared to when it lies in the floor. In

*Corresponding author: E-mail: satar.mahdevari@aut.ac.ir

Vol. 16, No. 46, Spring 2026, Pages 17-30

Journal of Analytical and Numerical Methods in Mining Engineering

Journal home page: http://anm.yazd.ac.ir/

other words, the presence of a coal seam at the tunnel floor intensifies the spread of the plastic zone, which in turn increases the risk of floor instability and heaving in both the tunnels and the bifurcated intersection.

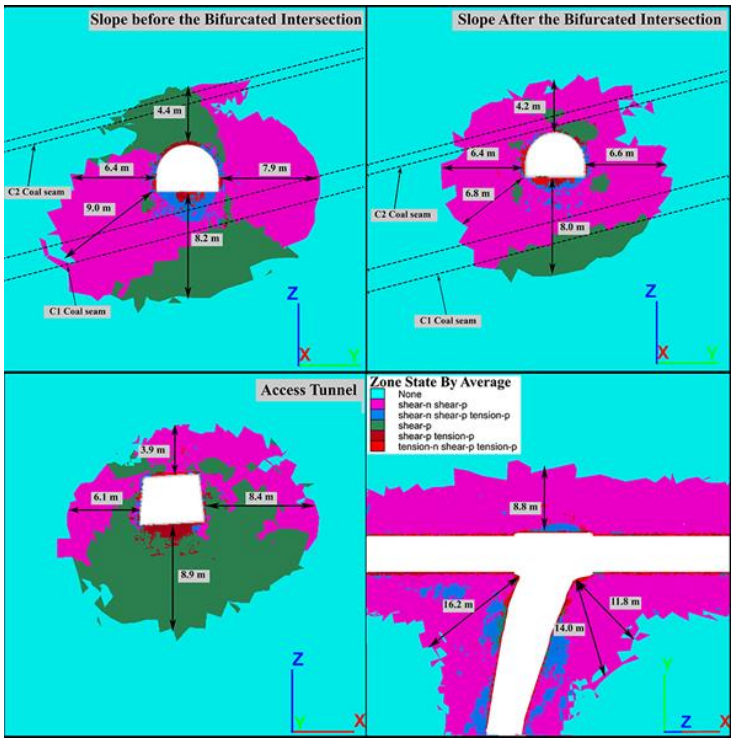

Fig. 5. Plastic zone at 20-meter distances from the center of bifurcated intersection

Considering the influence of input parameters on the results of the numerical model, this study investigates the effect of variations in three key input parameters—namely, deformation modulus, internal friction angle, and tunnel depth—on the maximum vertical displacement of the intersection roof. It is evident that in all cases, an increase in the deformation modulus and internal friction angle leads to a reduction in vertical displacements in the numerical model. Additionally, as the tunnel depth increases, the maximum displacement also increases, resulting in a decrease in the stability of the intersection.

To address excessive displacements and intersection instabilities in this mine, several practical measures are recommended. To control floor heave in tunnels, it is proposed to excavate tunnels with an inverted arch or modify the tunnel cross-section to a circular shape, accompanied by the installation of a floor support system. To manage displacements caused by access tunnel excavation, reducing the excavation step size is suggested to control the induced stresses around the intersection. Additionally, to mitigate deformations resulting from stress concentration, studying the behavior of tunnels with modified cross-sections—particularly circular profiles—is recommended. Implementing partial-face excavation instead of full-face excavation in the intersection zone may also be an effective approach to enhance the stability of bifurcated junctions.

References

[1] Chortis, F., & Kavvadas, M. Three-Dimensional Numerical Analyses of Perpendicular Tunnel Intersections. Geotechnical and Geological Engineering, 39(3), 1771-1793. (2020)

[2] Tan, Z., Zhou, Z., Kong, H., Zhao, B., & Zhao, J. Single excavation face method for super-large-span bifurcated tunnels. Proceedings of the Institution of Civil Engineers - Geotechnical Engineering, 1-13. (2021)

Vol. 16, No. 46, Spring 2026, Pages 17-30

Journal of Analytical and Numerical Methods in Mining Engineering

Journal home page: http://anm.yazd.ac.ir/

[3] Wang, J., Cao, A., Li, Z., et al. Mechanical Behavior and Excavation Optimization of a Small Clear-Distance Tunnel in an Urban Super Large and Complex Underground Interchange Hub. Applied Sciences, 13(1). (2022)

[4] Singh, R. N., Porter, I., & Hematian, J. Finite element analysis of three-way roadway junctions in longwall mining. International Journal of Coal Geology, 45(2-3), 115-125. (2001)

[5] Hsiao, F. Y., Wang, C. L., & Chern, J. C. Numerical simulation of rock deformation for support design in tunnel intersection area. Tunnelling and Underground Space Technology, 24(1), 14-21. (2009)

[6] Liu, X., & Wang, Y. Three Dimensional Numerical Analysis of Underground Bifurcated Tunnel. Geotechnical and Geological Engineering, 28(4), 447-455. (2010)

[7] Guo, Z., Shi, J., Wang, J., Cai, F., & Wang, F. Double-directional control bolt support technology and engineering application at large span Y-type intersections in deep coal mines. Mining Science and Technology (China), 20(2), 254-259. (2010)

[8] Li, G., He, M., Zhang, G., & Tao, Z. Deformation mechanism and excavation process of large span intersection within deep soft rock roadway. Mining Science and Technology (China), 20(1), 28-34. (2010)

[9] Lin, P., Zhou, Y., Liu, H., & Wang, C. Reinforcement design and stability analysis for large-span tailrace bifurcated tunnels with irregular geometry. Tunnelling and Underground Space Technology, 38, 189-204. (2013)

[10] Nik, M. G., & Farahani, A. F. Assessment the Stability of Tunnels in Y Shaped Intersections with Regard to the Intersection Angles, Case Study: Penstock Tunnels of Rudbar Dam. Amirkabir Journal of Civil Engineering, 48(2). (2016)

[11] Golshani, A., Joneidi, M., & Majidian, S. 3D numerical modeling for construction of tunnels intersections- case study of Hakim tunnel. Japanese Geotechnical Society Special Publication, 2(43), 1523-1527. (2016)

[12] Liu, H.-l., Li, S.-c., Li, L.-p., & Zhang, Q.-q. Study on deformation behavior at intersection of adit and major tunnel in railway. KSCE Journal of Civil Engineering, 21(6), 2459-2466. (2017)

[13] Zhou, D., Ding, W., Xie, D., & Chen, S. Reinforcement Analysis of Bifurcated Highway Tunnels with Large Section of Different Surrounding Rock Grades in Tiger Leaping Gorge. IOP Conference Series: Materials Science and Engineering, 741(1). (2020)

[14] Gkikas, V. I., & Nomikos, P. P. Primary Support Design for Sequentially Excavated Tunnel Junctions in Strain-Softening Hoek–Brown Rock Mass. Geotechnical and Geological Engineering, 39(3), 1997-2018. (2020)

[15] Xie, S., Wu, Y., Chen, D., Liu, R., Han, X., & Ye, Q. Failure analysis and control technology of intersections of large-scale variable cross-section roadways in deep soft rock. International Journal of Coal Science & Technology, 9(1). (2022)

[16] Xu, H., Zhang, Y., Yang, J., et al. Study on the Constant Resistance Coupling Support Technology for Rock Column at the Intersection Point of Deep Soft Rock Large Section Roadway: A Case Study in China. Shock and Vibration, 2022, 1-12. (2022)

[17] Sun, X.-m., Qi, Z.-m., Zhang, Y., Miao, C.-y., Zhao, C.-w., & He, M.-c. Failure mechanism and control countermeasures of surrounding rock at deep large section chamber intersection in the Wanfu Coal Mine. Journal of Mountain Science, 20(7), 2058-2075. (2023)

[18] Jiang, J., Tao, R., Hesham El Naggar, M., Liu, H., & Du, X. Seismic performance and vulnerability analysis for bifurcated tunnels in soft soil. Computers and Geotechnics, 167. (2024)

[19] (IRITEC), (2003). Tabas Coal Mine Project, detailed design report (Vol. 1, pp. 464).

[20] Mahdevari, S., Shahriar, K., Sharifzadeh, M., & Tannant, D. D. Stability prediction of gate roadways in longwall mining using artificial neural networks. Neural Computing and Applications, 28(11), 3537-3555. (2016)

[21] Tabas engineering technical. office. (2023). engineering report.

*Corresponding author: E-mail: satar.mahdevari@aut.ac.ir